Pseudospin-doublet bands and Gallagher Moszkowski doublet bands in ^{100}Y

E. H. Wang,[1] J. H. Hamilton,[1] A. V. Ramayya,[1] C. J. Zachary,[1] A. Lemasson,[2] A. Navin,[2] M. Rejmund,[2] S. Bhattacharyya,[3] Q. B. Chen,[4] S. Q. Zhang,[4] J. M. Eldridge,[1] J. K. Hwang,[1] N. T. Brewer,[1,*] Y. X. Luo,[1,5] J. O. Rasmussen,[5] S. J. Zhu,[6] G. M. Ter-Akopian,[7] Yu. Ts. Oganessian,[7] M. Caamaño,[8] E. Clément,[2] O. Delaune,[2] F. Farget,[2] G. de France,[2] and B. Jacquot[2]

[1]*Department of Physics and Astronomy, Vanderbilt University, Nashville, Tennessee 37235, USA*
[2]*GANIL, CEA/DRF - CNRS/IN2P3, Bd Henri Becquerel, BP 55027, F-14076 Caen, Cedex 5, France*
[3]*Variable Energy Cyclotron Centre, 1/AF Bidhan Nagar, Kolkata 700064, India*
[4]*State Key Laboratory of Nuclear Physics and Technology, School of Physics, Peking University, Beijing 100871, People's Republic of China*
[5]*Lawrence Berkeley National Laboratory, Berkeley, California 94720, USA*
[6]*Department of Physics, Tsinghua University, Beijing 100084, People's Republic of China*
[7]*Joint Institute for Nuclear Research, RU-141980 Dubna, Russian Federation*
[8]*USC, Universidad de Santiago de Compostela, E-15706 Santiago de Compostela, Spain*

(Received 25 November 2020; accepted 16 February 2021; published 2 March 2021)

New transitions in neutron-rich ^{100}Y have been identified in a ^{9}Be + ^{238}U experiment with mass and Z gates to provide full fragment identification. These transitions and high spin levels of ^{100}Y have been investigated by analyzing the high statistics γ-γ-γ and γ-γ-γ-γ coincidence data from the spontaneous fission of ^{252}Cf at the Gammasphere detector array. Two new bands, 14 new levels, and 23 new transitions have been identified. The $K^{\pi} = 4^{+}$ new band decaying to a 1s isomeric state is assigned to be the high-K Gallagher-Moszkowski (GM) partner of the known $K^{\pi} = 1^{+}$ band, with the $\pi 5/2[522] \otimes \nu 3/2[411]$ configuration. This 4^{+} band is also proposed to be the pseudospin partner of the new $K^{\pi} = 5^{+}$ band with a 5^{+} $\pi 5/2[422] \otimes \nu 5/2[413]$ configuration, to form a $\pi 5/2[422] \otimes \nu[312\ 5/2, 3/2]$ neutron pseudospin doublet. Constrained triaxial covariant density-functional theory and quantal particle rotor model calculations have been applied to interpret the band structure and available electromagnetic transition probabilities and are found to be in good agreement with experimental values.

DOI: 10.1103/PhysRevC.103.034301

I. INTRODUCTION

In the mass region $A \approx 100$, the shape transition and shape coexistence of the neutron-rich nuclei have long been of interest [1,2]. In this region, there exists a shell closure effect with $Z = 40$ and $N = 56$ spherical subshells and a sudden onset of large ground-state axially symmetric deformation for $N \geqslant 60$ occurs in the Sr ($Z = 38$), Y ($Z = 39$), and Zr ($Z = 40$) isotopes [2]. Thus, it is reasonable to consider the odd-odd ^{100}Y with $Z = 39$ and $N = 61$ to have a large quadrupole deformation.

The pseudospin is one of the current interests in nuclear study. In this concept, a pair of single-particle orbitals with quantum numbers $(n-1,\ l+2,\ j = l+3/2)$ and $(n,\ l,\ j = l+1/2)$ lie very close in energy. They can be labeled as a pseudospin doublet with quantum numbers $(\tilde{n} = n-1,\ \tilde{l} = l+1,\ \tilde{j} = l \pm 1/2)$. In the deformed case, the Nilsson states labeled by the asymptotic quantum numbers $[Nn_z\Lambda]\Omega$ have pseudo-Nilsson equivalents $[\tilde{N}\tilde{n}_z\tilde{\Lambda}]\tilde{\Omega}$, where $\tilde{N} = N-1$, $\tilde{n}_z = n_z$, $\tilde{\Lambda} = \Lambda \pm 1$, and $\tilde{\Omega} = \Omega = \tilde{\Lambda} + \tilde{\Sigma}$, where $\tilde{\Sigma} = \pm 1/2$. In the axially symmetric pseudo-Nilsson scheme, $\tilde{\Lambda}$, $\tilde{\Sigma}$, and $\tilde{\Omega}$ are good quantum numbers at all deformations [3]. In the A ≈ 100 region, pseudospin bands were reported in ^{108}Tc [4].

In this paper, we report the new high spin structure of ^{100}Y with identification of three new bands and the extension of a previously reported band [5,6]. Pseudospin doublet and Gallagher-Moszkowski (GM) doublet bands [7] are proposed in this nucleus. The constrained triaxial covariant density-functional theory and quantal particle rotor model calculations were performed and compared favorably with such assignments.

II. EXPERIMENTAL METHOD

Two complementary methods have been used to investigate the level structure of Y isotopes, which include (i) ^{9}Be + ^{238}U reaction in inverse kinematics with the unambiguous identification of the mass (A) and the proton number (Z) of the emitting fission fragment, using a large acceptance spectrometer for in-beam measurements, and (ii) the high-fold γ data from spontaneous fission of a ^{252}Cf source. These methods have allowed us to identify new transitions and extend the level schemes to higher spins of very-neutron-rich nuclei. In

*Present address: Physics Division, Oak Ridge National Laboratory, Oak Ridge, Tennessee 37831, USA.

the present work the new transitions identified using (A, Z) gated "singles" prompt γ-ray spectroscopy did not require knowledge of the spectroscopic information of the complementary fragment.

The first experimental measurements were performed at GANIL using a ^{238}U beam at 6.2 MeV/u, with an intensity of 0.2 pnA, impinging on a 10-μm-thick ^{9}Be target. The inverse kinematics used in this work with forward focused fission fragments have a large velocity, resulting in both an efficient detection and isotopic identification in the spectrometer. A single magnetic-field setting of the large-acceptance spectrometer VAMOS++ [10], possessing a momentum acceptance of around ±20%, placed at 20° with respect to the beam axis, was used to identify the fission fragments. The detection system (1×0.15 m^2) at the focal plane of the spectrometer was composed of (i) a multiwire parallel plate avalanche counter (MWPPAC), (ii) two drift chambers (x, y), (iii) a segmented ionization chamber (ΔE), and (iv) 40 silicon detectors arranged in a wall structure (E_r). The time of flight (TOF) was obtained by using the signals from the two MWPPACs, one located after the target and the other at the focal plane (flight path ≈7.5 m). The parameters measured at the focal plane [(x, y), ΔE, E_r, TOF] along with the known magnetic field were used to determine, on an event-by-event basis, the mass number A, charge state q, atomic number Z, and velocity vector after the reaction for the detected fragment. Isotopic identifications of elements were made up to $Z = 63$ with a mass resolution of $\Delta A/A \approx 0.4\%$ [11]. The prompt γ rays were measured in coincidence with the isotopically identified fragments, using the EXOGAM array [12] consisting of 11 Compton-suppressed segmented clover HpGe detectors placed 15 cm from the target. The velocity of the fragment along with the angle of the segment of the relevant clover detector were used to obtain the γ-ray energy in the rest frame of the emitting fragment. Errors on the γ-ray energies of the strong transitions are 0.5 keV, while for the weak transitions it could be as much as 1 keV. As compared with the results presented in Ref. [11] for the Zr isotopes the present work is the result of further improvements in the analysis, especially improving the Z identification, and also involves a larger data set.

Second, the SF of ^{252}Cf experimental work was done by examining the prompt γ rays emitted. The γ rays were detected with the Gammasphere array at the Lawrence Berkeley National Laboratory (LBNL). A 62 μCi ^{252}Cf source was sandwiched between two iron foils of 10 mg/cm^2, which were used to stop the fission fragments and eliminate the need for a Doppler correction. A plastic (CH) ball of 7.62 cm in diameter surrounding the source was used to absorb β rays and conversion electrons, as well as to partially moderate and absorb fission neutrons. A total of 5.7×10^{11} γ-γ-γ and higher-fold γ events, and 1.9×10^{11} γ-γ-γ-γ and higher-fold γ coincident events were recorded. These γ coincident data were analyzed by using the RADWARE software package [13]. Both the triple and fourfold coincidence data have a manual selected low-energy cut from the software at ≈33 keV. The binning of the triple coincidence data is about 0.67 keV/channel at the low-energy end. This value increases with the energy. The fourfold coincidence data have a fixed binning at 1.33 keV/channel. The energy calibration error for the ^{252}Cf data is about 0.1 keV, while the fitting error for a single strong peak in the gated spectrum is usually much lower. However, in some other common cases, some weak or unknown contaminations in the gated spectra would enlarge the energy error which is hard to evaluate accurately. More experimental setup details can be found in Ref. [2].

III. EXPERIMENTAL RESULTS

The level scheme of ^{100}Y is shown in Fig. 1. The ground state of ^{100}Y was assigned as 1^- or 2^- in β-decay work [5]. A 1^+ $\pi 5/2[422] \otimes \nu 3/2[411]$ band was reported in Refs. [5,6]. In the current work, this band (1) has been extended up to 10^+ with three new transitions and levels. The new bands (2) and (3) identified in the present work could decay to the ground state or a 145(15) keV 4^+ 0.94 s isomeric state reported in Refs. [8,9,15]. Since no transitions in bands (2) and (3) were identified in the previous β-decay study [5], these bands are proposed to decay to the 4^+ isomeric state.

Figure 2 shows a A- and Z-gated spectrum on ^{100}Y from ^{238}U + ^{9}Be induced fission work. In this spectrum, the previously reported transitions in band (1) and new transitions in bands (2) and (3) can be clearly seen. Note that the 125.0, 230.3, 310.8 keV transitions are not identified in the ^{252}Cf SF data so that they are not placed in the level scheme. It is worth noting that there is a strong 125.3 keV transition in ^{99}Y with one neutron number less than ^{100}Y. However, since the strong 128.4 keV transition in ^{101}Y, the 287.2 keV transition in ^{100}Sr, the 212.6 keV transition in ^{100}Zr are not clearly seen, this spectrum is clean to Z and higher mass gate. Note that the transitions in band (2) are identical to a band reported in ^{102}Nb. Since the intensities of the transitions leaking through $\Delta M = 2$ gates should be very small and no such leakage is seen in any other A/Z gated spectra in the previous work, the transitions in band (2) in the ^{100}Y A- and Z- gated spectrum belong to ^{100}Y rather than ^{102}Nb.

Figure 3(a) shows a γ ray coincidence spectrum by triple gating on three known transitions in band (1) from ^{252}Cf spontaneous fission data. The 257.6, 273.5, and 318.1 keV new transitions in band (1) can be seen. Figure 3(b) shows a γ-ray coincidence spectrum by gating on two transitions in the strongly populated $3n$ fission partner ^{149}Pr and the strong 162.1 keV transition identified in the A/Z gated spectrum in Fig. 2. Despite the contamination, transitions in ^{101}Y (the $2n$ partner of ^{149}Pr), which originate from the 163.3 keV transition in ^{101}Y, the 193.4, 223.7, 253.1, and 282.9 keV new transitions identified in the A/Z gated ^{100}Y spectrum are clearly seen. The 223.7, 253.1, 282.9, 476.9, and 536.5 keV transitions in band (2) are also seen in the coincidence spectrum gating on a strong transition in ^{149}Pr and the 162.1 and 193.4 keV transitions in Fig. 3(c). These coincidence spectra from ^{252}Cf SF further confirm that the somewhat broadened peak around 160 keV in Fig. 2 contains two components of 158 and 162 keV. Figure 4(a) shows a γ-ray coincidence spectrum by double gating on a strong transition in band (3) of ^{100}Y and a ^{149}Pr fission partner transition. The correlated 179, 209, 239, 271, 299, 388, 449, 511, and 570 keV transitions in band (3) can be seen. These transitions are also confirmed

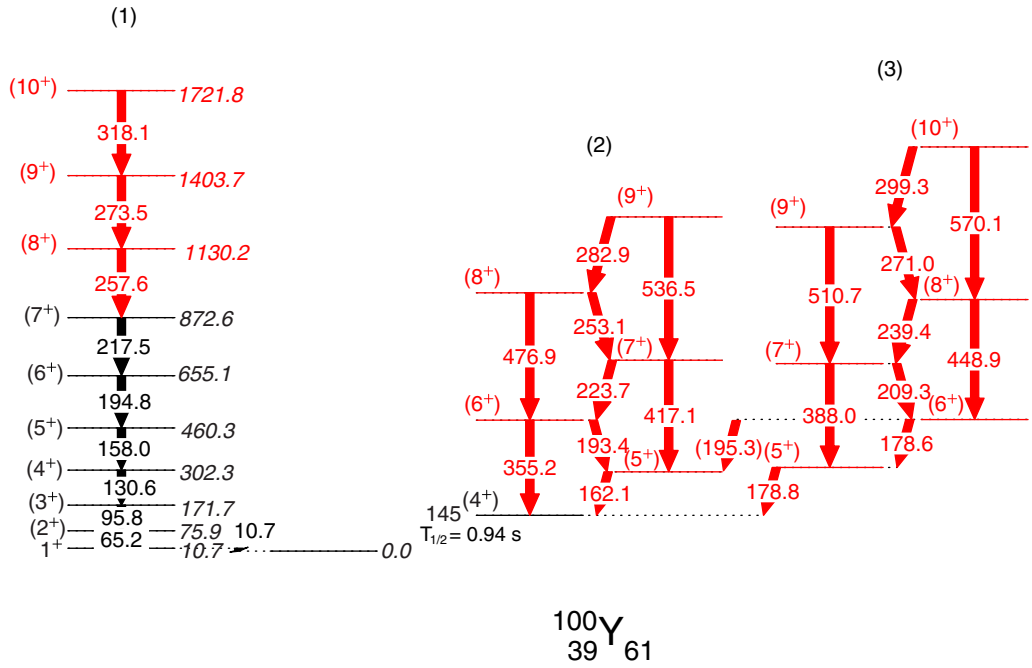

FIG. 1. The new level scheme of ^{100}Y obtained in the present work. New transitions and levels are labeled in red. The 10.7 keV transition is not observed in the current work but is reported in Ref. [5]. Previous rotational band (1) was reported in Ref. [6]. The 145 keV isomer was reported in Refs. [8,9].

in the 178.6 and 178.8 keV double coincidence spectrum in Fig. 4(b).

IV. DISCUSSION

Band (1) was assigned to have a 1^+ $\pi 5/2[422] \otimes \nu 3/2[411]$ configuration [5,6]. Such a configuration is adopted in the current work. The neutron pairing gap and proton pairing gap of this state are proposed to drop down [5], which results in the moments of inertia very close to a rigid body one (Fig. 5). Note that the $M1$ transition energies of the same spins in bands (1), (2), and (3) are very close, e.g., 158 and 162 keV from 5^+ to 4^+, 195, 193 and one of the 179 keV from 6^+ to 5^+. Therefore, the moments of inertias in these two bands are also very close to rigid body. However, only band (1) is shown in Fig. 5 because the values in band (2) and (3) would be too close to be seen in a figure.

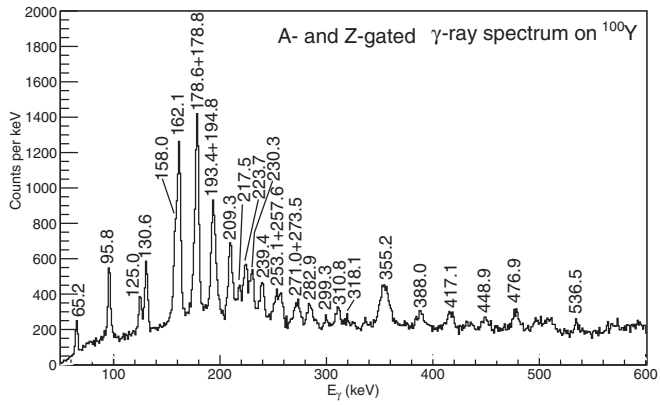

FIG. 2. A- and Z-gated spectrum on ^{100}Y in ^{238}U + ^{9}Be data.

Experimental measurements on $Z = 36$–40 isotopes revealed a sudden onset of deformation at $N \approx 60$. For yttrium isotopes, deformation was small for $N = 48$–58 and shape coexistence was reported for $N = 59$ [9]. Then, the deformation suddenly changes to a higher value ($\beta_2 \approx 0.4$) for $N = 60$, 62 with almost no triaxiality. Cheal *et al.* reported a tentative spin 3 for the ground state of ^{100}Y with 0.39(4) β_2 deformation from laser spectroscopy [16]. Baczynska *et al.* reassigned this state as a 0.35(4) β_2 deformation, spin 4 isomeric state by using a similar experimental approach [9]. A probable 4^+ $\pi 5/2[422] \otimes \nu 3/2[411]$ configuration was suggested from comparison of g factors between experiment and theory [9]. Similar and regular energy spacing with no signature splitting in bands (2) and (3) indicate a large rigid deformation, which is consistent with systematics. Note that ^{99,101}Y are both proposed to have large quadrupole deformation [9,16,17]. As discussed in the previous section, the bandhead of band (2) is proposed to be the 145(15) keV 4^+ isomer. The configurations of these bands would be $4^+\pi 5/2[422] \otimes \nu 3/2[411]$ and 5^+ $\pi 5/2[422] \otimes \nu 5/2[413]$, respectively, according to the Nilsson orbitals in this region. Bandheads of (2) and (3) would form a $\pi 5/2[422] \otimes \nu[312\ 5/2, 3/2]$ neutron pseudospin doublet. Bands (1) and (2) would form a GM doublet and originate from the Gallagher Moskowski interaction, in which the intrinsic spins of proton and neutron are coupled parallel and antiparallel to get low $K = |\Omega_\pi - \Omega_\nu|$ and high $K = \Omega_\pi + \Omega_\nu$. In the neighboring ^{98}Sr and ^{99}Y isotopes, this GM structure has also been observed [17–19].

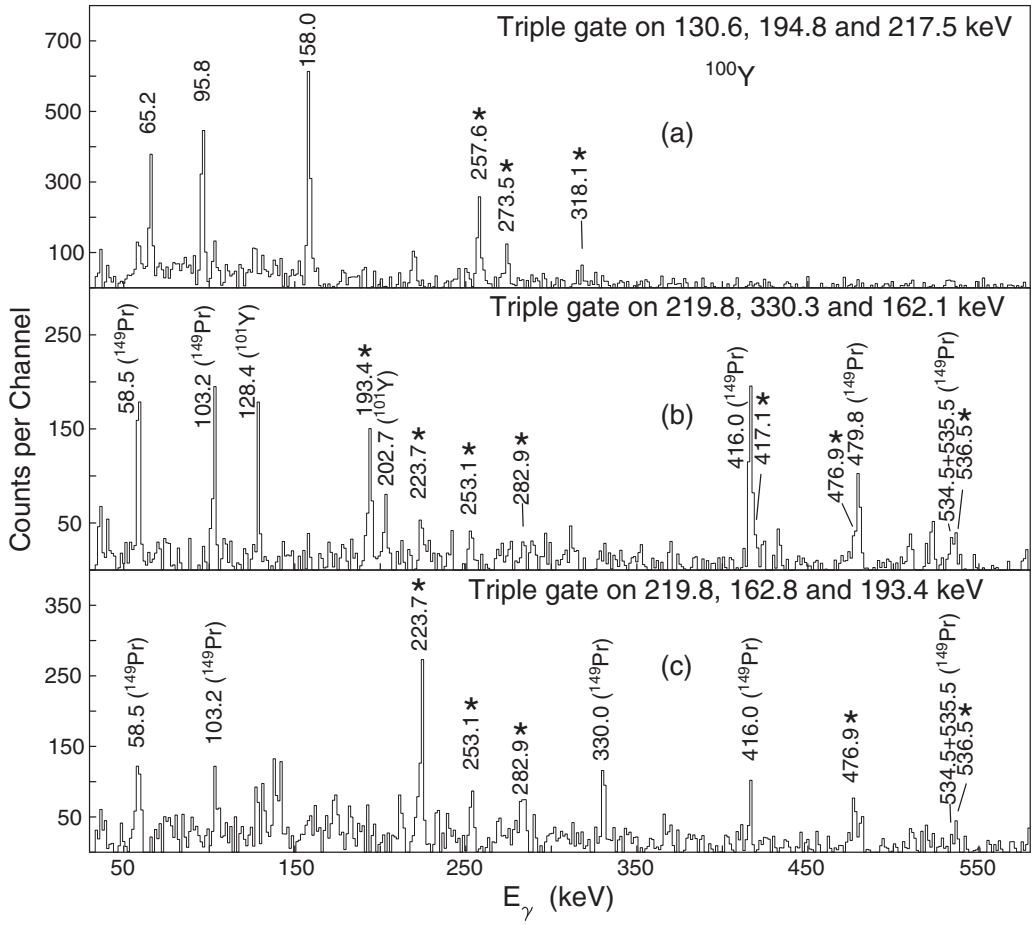

FIG. 3. Partial γ-ray coincidence spectrum obtained from ^{252}Cf spontaneous fission data. Part (a) shows a triple gated spectrum on the 130.6, 194.8, and 217.5 keV transitions in band (1). Part (b) depicts a triple gate on the 219.8 and 330.3 keV transitions in ^{149}Pr fission partner and 162.1 keV transitions in ^{100}Y. Part (c) denotes a triple gate on the 219.8 keV transition in the ^{149}Pr fission partner and the 162.1 and 193.4 keV transitions in ^{100}Y. Note that ^{101}Y has a 163.3 keV transition to bring in ^{101}Y contamination transitions in part (b). Transitions marked with * are new.

A. Constrained covariant density-functional theory calculations

To understand the nature of the observed band structure in ^{100}Y, constrained triaxial covariant density-functional theory (CDFT) calculations [20–25] were first performed to obtain the potential-energy surface (PES) to search for the possible configurations and deformation parameters. Subsequently, with the obtained configurations and deformations, quantal particle rotor model (PRM) [26–34] calculations were carried out to reproduce the energy spectra and electromagnetic transition probabilities and investigate the angular-momentum geometries for bands (1), (2), and (3).

In the constrained triaxial CDFT calculations, the point-coupling energy density functional PC-PK1 [35] in the particle-hole channel is adopted, while the pairing correlations in the particle-particle channel are neglected. The neglecting of the pairing correlations in the CDFT calculations is consistent with the fact that the extracted experimental moments of inertia of the three bands are very close to a rigid body one, as shown in Fig. 5 and the discussion above. The solutions of the equation of motion for the nucleons are accomplished by an expansion of the Dirac spinors in a set of three-dimensional harmonic-oscillator basis functions in Cartesian coordinates with 12 major shells. The PES is obtained by constraining the (β_2, γ) deformation parameters in the intervals $\beta_2 \in [0.0, 0.8]$ and $\gamma \in [0^\circ, 60^\circ]$, with step sizes $\Delta\beta_2 = 0.05$ and $\Delta\gamma = 6^\circ$, respectively.

In Fig. 6, the PES in the β_2-γ plane for ^{100}Y calculated by the constrained triaxial CDFT is shown. It shows that the minimum of the PES (ground state, labeled by the dot at the bottom) locates at $(\beta_2 = 0.45, \gamma = 0^\circ)$, which corresponds to a large prolate shape. Meanwhile, it is interesting to note that there is a local minimum (labeled by the square on the left) around at $(\beta_2 = 0.32, \gamma = 60^\circ)$. However, its energy is higher than that of the ground state by about 1.0 MeV; even this value is much larger than that of the bandhead energy of band (3), 334 keV. Thus it can be understood that the band built on this oblate state has not been observed in the present experiment.

It is found that the valence nucleon configuration of the ground state of ^{100}Y is expressed as spherical orbits, $\pi(1g_{9/2})^5 \otimes \nu(2d_{5/2})^3(1g_{7/2})^4(1h_{11/2})^4$, which has a positive parity. Considering that the $2d_{5/2}$ and $1g_{7/2}$ orbitals are a pair of pseudopartners with admixtures that are too large to be distinguished, and the paired orbits have no

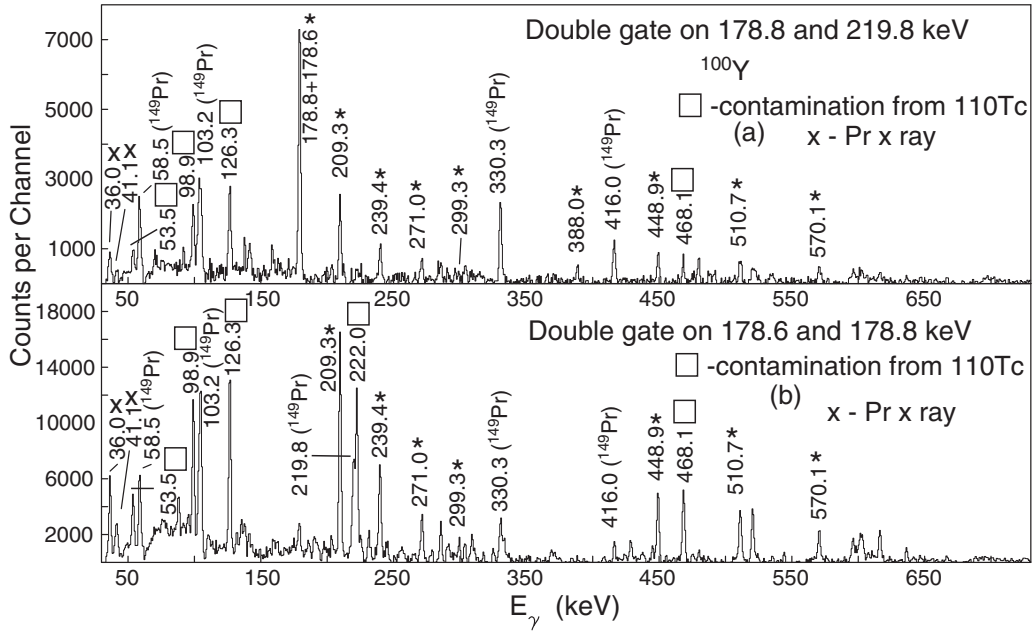

FIG. 4. Partial γ-ray coincidence spectrum obtained from ^{252}Cf spontaneous fission data. Panels (a) and (b) show double gated spectra on 178.8 keV transition in ^{100}Y and 219.8 keV transition in ^{149}Pr, and 178.6 and 178.8 keV transitions in ^{100}Y, respectively. All the ^{100}Y transitions in these two spectra are new and are labeled with an asterisk. Contamination transitions from ^{110}Tc marked in these two spectra come from the coincidence of 222.0-178.3-178.9 keV transitions in ^{110}Tc. Details of the level scheme of ^{110}Tc can be found in Ref. [14].

contributions to the total angular momentum, the ground-state configuration can be rewritten as $\pi(1g_{9/2})^1 \otimes \nu(2d_{5/2})^1$ or $\pi(1g_{9/2})^1 \otimes \nu(1g_{7/2})^{-1}$. The former corresponds to the configuration $\pi 5/2[422] \otimes \nu 3/2[411]$ and will be assigned to bands (1) and (2), and the latter $\pi 5/2[422] \otimes \nu 5/2[413]$ to band (3). Such configuration assignments are consistent with the previous investigations in Refs. [5,6,9] and the systematic analyses discussed above and will be examined and confirmed by the following comparisons between the PRM calculated results and the experimental observations.

B. Particle-rotor model calculations

With the configurations and deformation parameters obtained from the constrained triaxial CDFT calculations, it is straightforward to perform the PRM calculations to study the energy spectra, the electromagnetic transition probabilities, and the angular-momentum geometries for the observed bands (1), (2), and (3) in ^{100}Y.

The many-particle-many-hole PRM calculations have been carried out for bands (1) and (2) with the configurations $\pi(1g_{9/2})^5 \otimes \nu(2d_{5/2})^3$, and for band (3) with

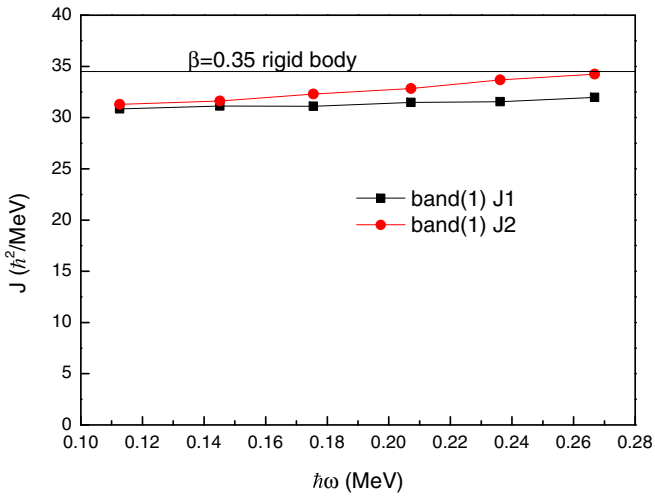

FIG. 5. Moments of inertia ($J^{(1)}$ and $J^{(2)}$) of band (1) in ^{100}Y.

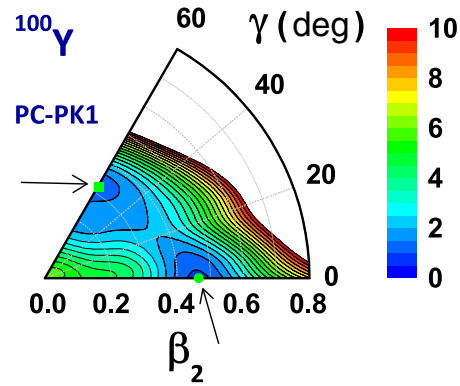

FIG. 6. Potential-energy surface in the β_2-γ plane ($0 \leqslant \beta_2 \leqslant 0.8$, $0 \leqslant \gamma \leqslant 60^\circ$) for the ground-state configuration of ^{100}Y in constrained triaxial CDFT calculations with the PC-PK1 effective interaction. All energies are normalized with respect to the energy of the absolute minimum (in MeV) indicated by the dot and arrow. The energy separation between each contour line is 0.5 MeV.

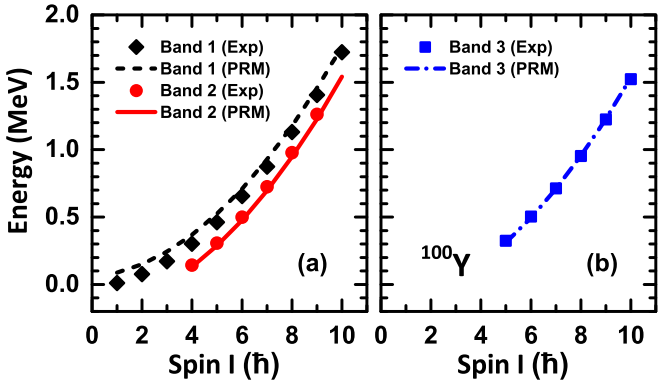

FIG. 7. The energy spectra for bands (1), (2), and (3) calculated by PRM in comparison with the data.

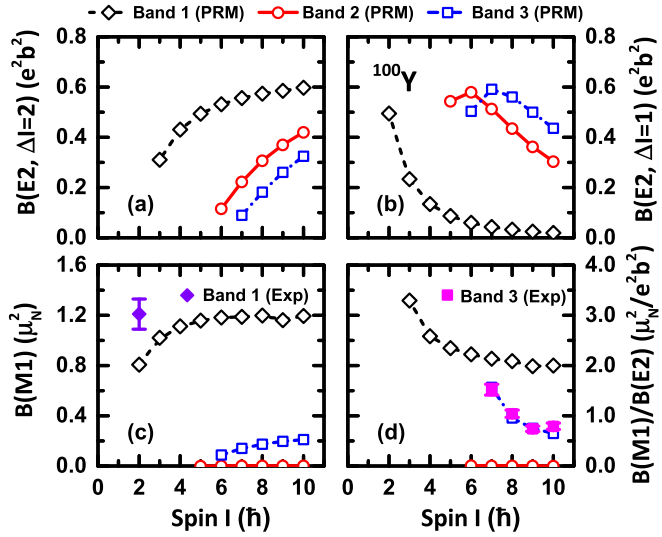

FIG. 8. The in-band reduced electromagnetic transition probabilities $B(E2,\ \Delta I=2)$, $B(E2,\ \Delta I=1)$, and $B(M1)$, and the $B(M1)/B(E2)$ ratios of bands (1), (2), and (3) calculated by the PRM in comparison with the available data. The experimental $B(M1)$ value for the 2^+ state in band (1) is extracted from the β decay data [38], as shown in the left bottom of panel (c) for comparison. The experimental value for $B(M1)/B(E2)$ value obtained in the present work for band (3) is also included in panel (d) for comparison.

$\pi(1g_{9/2})^5 \otimes \nu(1g_{7/2})^5$. In both calculations, the deformation parameters are used as $(\beta_2 = 0.45, \gamma = 0^\circ)$, obtained from the constrained triaxial CDFT calculations. With the deformation parameters, the single-j shell Hamiltonian coupling parameter can be calculated by [36]

$$C = \left(\frac{123}{8}\sqrt{\frac{5}{\pi}}\right)\frac{2N+3}{j(j+1)}A^{-1/3}\beta_2, \qquad (1)$$

where N denotes the number of oscillator quanta. The moments of inertia are chosen to be $\mathcal{J} = 20.0\ \hbar^2/\text{MeV}$. In the electromagnetic transition probabilities calculation, the empirical intrinsic quadrupole moment $Q_0 = (3/\sqrt{5\pi})R_0^2 Z\beta_2$ with $R_0 = 1.2A^{1/3}$ fm, the gyromagnetic ratio $g_R = Z/A = 0.39$, $g_\pi(g_{9/2}) = 1.26$, $g_\nu(d_{5/2}) = -0.46$, and $g_\nu(g_{7/2}) = 0.70$ are adopted [37].

In Fig. 7, the energy spectra for bands (1), (2), and (3) calculated by PRM are shown in comparison with the data. It is seen that the PRM results excellently agree with the data, which confirms the configuration assignments for these three bands. For bands (1) and (2), they are separated by a nearly constant value (≈150 keV) over the whole spin region. This can be understood, in the following, that they are built on the different bandheads, that the intrinsic spins of proton and neutron are coupled in parallel and antiparallel to low $K = |\Omega_\pi - \Omega_\nu| = 1\hbar$ and high $K = \Omega_\pi + \Omega_\nu = 4\hbar$. For bands (2) and (3), their energy differences are rather small (within 20 keV). This is because they are built on a pair of nearly degenerate pseudospin partner configurations $\nu(2d_{5/2})$ and $\nu(1g_{7/2})$. Here, we should mention that the present PRM cannot give this energy difference since the two calculations are carried out separately with different model spaces.

The in-band reduced electromagnetic transition probabilities $B(E2,\ \Delta I = 2)$, $B(E2,\ \Delta I = 1)$, and $B(M1)$, and the $B(M1)/B(E2)$ ratios of bands (1), (2), and (3) calculated by the PRM are presented in Fig. 8, together with the available data. The $B(M1)$ value in band (1) extracted from beta decay [38] and the $B(M1)/B(E2)$ ratios extracted from the current work assume pure $M1$ for the $\Delta I = 1$ transitions. Because of the identical transitions in ^{102}Nb [6] and the 416, 479, 535 keV transitions in the ^{149}Pr fission partner, it is difficult to obtain accurate transition intensities and $B(M1)/B(E2)$ ratios in band (2). Thus, such ratios in band (2) from experiment data are not provided in the present work. For the $B(E2,\ \Delta I = 2)$, it increases smoothly with spin. It is seen that it becomes smaller with the larger K, which is due to the Clebsch-Gordon coefficients $\langle I_i K 20 | I_f K\rangle$ $(I_i = I_f + 2)$ [39]. For the $B(E2,\ \Delta I = 1)$, contrary to $B(E2,\ \Delta I = 2)$, it decreases with spin. Moreover, it shows strong competitions with $B(E2,\ \Delta I = 2)$. Large $B(E2,\ \Delta I = 1)$ is accompanied by small $B(E2,\ \Delta I = 2)$, vice versa.

For the $B(M1)$, it is seen that the band (1) shows a large value ($\approx 1.2\ \mu_N^2$). This result is in good agreement with the experiment value of 2^+ state, as seen in Fig. 8(c), from β decay measurement [38]. This further supports the configuration assignment for band (1). However, one notes that its partner band (2) presents an almost vanished value. The reason can be understood from the value of the g factor and the coupling modes in these two bands. For the g factor, we have $g_\pi(g_{9/2}) - g_R = 0.87$ and $g_\nu(d_{5/2}) - g_R = -0.85$. As a consequence, for band (1), where proton and neutron are coupled in antiparallel, the $B(M1)$ values are enhanced. In contrast, for band (2) with the proton and neutron being parallel coupled, the $B(M1)$ values are reduced significantly. Similarly, as $g_\nu(g_{7/2}) - g_R = 0.31$ is small. The $B(M1)$ values of band (3) are small as well. Here, it is worth mentioning that, according to the PRM results, the in-band $\Delta I = 1$ transitions in bands (2) and (3) are dominated primarily by $E2$ transitions rather than $M1$ transitions. Therefore, it is highly expected that the angular distribution and the polarization asymmetry would

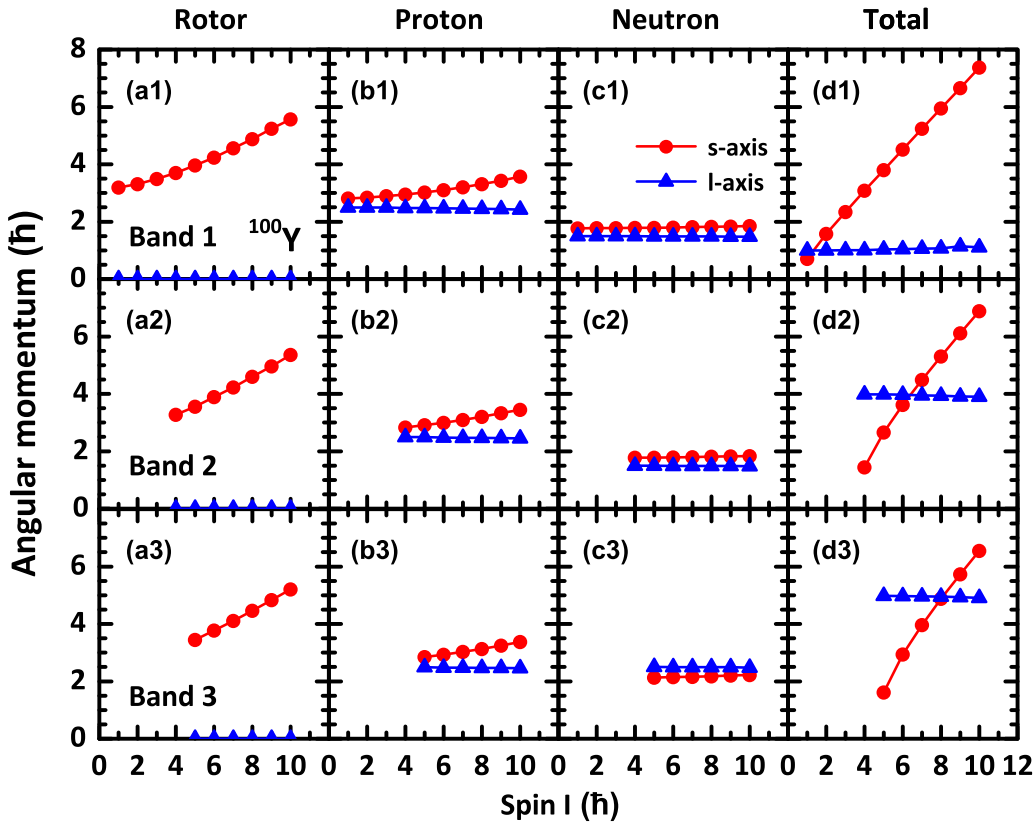

FIG. 9. The root mean square components of the angular momentum along the short (s, circles) and long (l, triangles) axes of the core $\boldsymbol{R}$, the proton $\boldsymbol{j}_\pi$, the neutron $\boldsymbol{j}_\nu$, and the total spin $\boldsymbol{I}$ calculated by PRM for bands (1), (2), and (3).

be measured for these transitions in the future experiments to identify their multipolarities.

For the $B(M1)/B(E2)$ ratio, it decreases with spin for bands (1) and (3), and almost vanishes for band (2). The former one is caused by the increase $B(E2)$, and the latter one by the vanished $B(M1)$, as seen in Figs. 8(a) and 8(c). The available experimental values of band (3) are reproduced by the PRM very well. This is further in favor of the configuration assignment for band (3).

The successes in reproducing the energy spectra and electromagnetic transition probabilities of the bands (1), (2), and (3) in ^{100}Y by PRM encourage us to investigate the corresponding angular-momentum geometries to learn the coupling modes in these three bands. In Fig. 9, the root mean square components along the short (s, circles) and long (l, triangles) axes of the core $\boldsymbol{R}$, the proton $\boldsymbol{j}_\pi$, the neutron $\boldsymbol{j}_\nu$, and the total spin $\boldsymbol{I}$ calculated by PRM for bands (1), (2), and (3) are thereby illustrated. Note that since the three bands are all prolate deformed, here the l axis is the symmetry axis, and the s axis is the axis that is perpendicular to the symmetry axis.

For the rotor, its rotational angular momentum aligns along the s axis for all three bands, and its l component vanishes as expected in axially deformed bands. As the total spin increases, R_s also increases gradually. For the $1g_{9/2}$ valence protons, they mainly align along the s axis. Its l component keeps almost a constant value with $\Omega_\pi = 5/2\hbar$. For the $2d_{5/2}$ valence neutrons in bands (1) and (2) and the $1g_{7/2}$ valence neutrons in band (3), the three components are very similar, and are almost constant. Note that the l component is $\Omega_\nu = 3/2\hbar$ in the former ones, and $\Omega_\nu = 5/2\hbar$ in the latter one. For the total spin, its s components linearly increase with spin, which is induced by the increases of the rotor and the valence protons. It is interesting to observe that its l component is quite different in the three bands. Namely, $K = 1\hbar$, $4\hbar$, and $5\hbar$ in bands 1, 2, and 3, respectively.

Therefore, according to the above angular-momentum geometry analyses, it is clearly seen that the protons and neutrons in the bands (2) and (3) are coupled in parallel to respectively get $K = \Omega_\pi + \Omega_\nu = 4\hbar$ and $5\hbar$, while they are antiparallel to get $K = |\Omega_\pi - \Omega_\nu| = 1\hbar$ in band (1). This strongly supports the GM doublet interpretation for bands (1) and (2), and the pseudospin doublet interpretation for bands (2) and (3). This observation provides solid experimental evidence for the coexistence of the GM doublet and pseudospin doublet bands in the same nucleus.

V. SUMMARY

In summary, the new transitions and levels in neutron-rich ^{100}Y have been identified by ^{9}Be + ^{238}U experiment with A and Z gate with fragment identification. The coincidence of these transitions have been investigated by analyzing the high-statistics γ-γ-γ and γ-γ-γ-γ coincidence data from the spontaneous fission of ^{252}Cf. Two new bands have been identified for the first time built on the isomer. The configurations

of the band structures in ^{100}Y have been assigned from the theoretical calculations.

Constrained triaxial CDFT calculations and quantal PRM calculations have been performed to explain the observed band structures. The obtained PES from the CDFT calculations suggests that the ^{100}Y has a large prolate deformed ground state with $\beta_2 = 0.45$. With the obtained deformation parameter and the configuration, the PRM calculations excellently reproduce the experimental energy spectra and the available electromagnetic transition probabilities for bands (1), (2), and (3). By analyzing the angular momentum geometries, it is confirmed that the $K = 4^+$ new band is a high-K GM partner of the known $K = 1^+$ band, with the $\pi 5/2[522] \otimes \nu 3/2[411]$ configuration, and is also proposed to be the pseudospin partner of the new $K = 5^+$ band with a $\pi 5/2[422] \otimes \nu 5/2[413]$ configuration, to form a $\pi 5/2[422] \otimes \nu[312\ 5/2, 3/2]$ neutron pseudospin doublet. This observation provides solid experimental evidence for the coexistence of the GM doublet and pseudospin doublet bands in a same nucleus.

ACKNOWLEDGMENTS

The work at Vanderbilt University and Lawrence Berkeley National Laboratory is supported by the US Department of Energy under Grant No. DE-FG05-88ER40407 and Contract No. DE-AC03-76SF00098. The work at Tsinghua University was supported by the National Natural Science Foundation of China under Grant No. 11175095. The work at JINR was supported by the Russian Foundation for Basic Research Grant No. 08-02-00089 and by the INTAS Grant No. 03-51-4496. The work at Peking University is supported by the Chinese Major State 973 Program No. 2013CB834400, the National Natural Science Foundation of China (Grants No. 11335002, No. 11375015, and No. 11461141002), and the China Postdoctoral Science Foundation under Grants No. 2015M580007 and No. 2016T90007. One of us (S.B.) acknowledges partial financial support through the LIA France-India agreement. We would like to thank J. Goupil, G. Fremont, L. Ménager, J. Ropert, C. Spitaels, and the GANIL accelerator staff for their technical contributions.

[1] J. Skalski, S. Mizutori, and W. Nazarewicz, Nucl. Phys. A **617**, 282 (1997).
[2] J. H. Hamilton *et al.*, Prog. Part. Nucl. Phys. **35**, 635 (1995).
[3] A. E. Stuchbery, J. Phys. G **25**, 611 (1999).
[4] Q. Xu *et al.*, Phys. Rev. C **78**, 064301 (2008).
[5] F. K. Wohn, J. C. Hill, J. A. Winger, R. F. Petry, J. D. Goulden, R. L. Gill, A. Piotrowski, and H. Mach, Phys. Rev. C **36**, 1118 (1987).
[6] J. K. Hwang *et al.*, Phys. Rev. C **58**, 3252 (1998).
[7] C. J. Gallagher, Jr. and S. A. Moszkowski, Phys. Rev. **111**, 1282 (1958).
[8] U. Hager *et al.*, Nucl. Phys. A **793**, 20 (2007).
[9] K. Baczynska *et al.*, J. Phys. G **37**, 105103 (2010).
[10] M. Rejmund *et al.*, Nucl. Instrum. Methods Phys. Res., Sect. A **646**, 184 (2011).
[11] A. Navin *et al.*, Phys. Lett. B **728**, 136 (2014).
[12] J. Simpson *et al.*, Acta Phys. Hung. New Ser.: Heavy Ion Phys. **11**, 159 (2000).
[13] D. C. Radford, Nucl. Instrum. Methods Phys. Res., Sect. A **361**, 297 (1995).
[14] Y. X. Luo *et al.*, Phys. Rev. C **74**, 024308 (2006).
[15] T. A. Khan *et al.*, Z. Phys. A: At. Nucl. (1975) **283**, 105 (1977).
[16] B. Cheal *et al.*, Phys. Lett. B **645**, 133 (2007).
[17] Y. X. Luo *et al.*, J. Phys. G **31**, 1303 (2005).
[18] M. L. Li *et al.*, Chin. Phys. Lett. **21**, 2147 (2004).
[19] R. A. Meyer *et al.*, Nucl. Phys. A **439**, 510 (1985).
[20] J. Meng, J. Peng, S. Q. Zhang, and S.-G. Zhou, Phys. Rev. C **73**, 037303 (2006).
[21] P. Ring, Prog. Part. Nucl. Phys. **37**, 193 (1996).
[22] D. Vretenar, A. Afanasjev, G. Lalazissis, and P. Ring, Phys. Rep. **409**, 101 (2005).
[23] J. Meng, H. Toki, S. Zhou, S. Zhang, W. Long, and L. Geng, Prog. Part. Nucl. Phys. **57**, 470 (2006).
[24] J. Meng, J. Y. Guo, Z. P. Li, H. Z. Liang, W. H. Long, Y. F. Niu, Z. M. Niu, J. M. Yao, Y. Zhang, P. W. Zhao *et al.*, Prog. in Phys. **31**, 199 (2011).
[25] *Relativistic Density Functional for Nuclear Structure*, edited by J. Meng (World Scientific, Singapore, 2016).
[26] S. Frauendorf and J. Meng, Nucl. Phys. A **617**, 131 (1997).
[27] J. Peng, J. Meng, and S. Q. Zhang, Phys. Rev. C **68**, 044324 (2003).
[28] S. Q. Zhang, B. Qi, S. Y. Wang, and J. Meng, Phys. Rev. C **75**, 044307 (2007).
[29] B. Qi, S. Q. Zhang, J. Meng, S. Y. Wang, and S. Frauendorf, Phys. Lett. B **675**, 175 (2009).
[30] Q. B. Chen, J. M. Yao, S. Q. Zhang, and B. Qi, Phys. Rev. C **82**, 067302 (2010).
[31] B. Qi, S. Q. Zhang, S. Y. Wang, J. Meng, and T. Koike, Phys. Rev. C **83**, 034303 (2011).
[32] A. D. Ayangeakaa, U. Garg, M. D. Anthony, S. Frauendorf, J. T. Matta, B. K. Nayak, D. Patel, Q. B. Chen, S. Q. Zhang, P. W. Zhao *et al.*, Phys. Rev. Lett. **110**, 172504 (2013).
[33] E. O. Lieder, R. M. Lieder, R. A. Bark, Q. B. Chen, S. Q. Zhang, J. Meng, E. A. Lawrie, J. J. Lawrie, S. P. Bvumbi, N. Y. Kheswa *et al.*, Phys. Rev. Lett. **112**, 202502 (2014).
[34] I. Kuti, Q. B. Chen, J. Timár, D. Sohler, S. Q. Zhang, Z. H. Zhang, P. W. Zhao, J. Meng, K. Starosta, T. Koike *et al.*, Phys. Rev. Lett. **113**, 032501 (2014).
[35] P. W. Zhao, Z. P. Li, J. M. Yao, and J. Meng, Phys. Rev. C **82**, 054319 (2010).
[36] S. Y. Wang, B. Qi, and S. Q. Zhang, Chin. Phys. Lett. **26**, 052102 (2009).
[37] P. Ring and P. Schuck, *The Nuclear Many Body Problem* (Springer Verlag, Berlin, 1980).
[38] H. Mach, F. K. Wohn, M. Moszyn'ski, R. L. Gill, and R. F. Casten, Phys. Rev. C **41**, 1141 (1990).
[39] A. Bohr and B. R. Mottelson, *Nuclear Structure* (Benjamin, New York, 1975), Vol. II.